Supplementary Information

Trapping sulfur in hierarchically porous, hollow indented carbon spheres: a high-performance cathode for lithium-sulfur batteries

Yijun Zhong,[ab] Shaofeng Wang,[ab] Yujing Sha,[ab] Meilin Liu,*[c] Rui Cai,[b] Li Li,[d] and Zongping Shao*[ade]

a. Jiangsu National Synergetic Innovation Center for Advanced Materials, State Key Laboratory of Materials-Oriented Chemical Engineering, Nanjing Tech University, No. 5 Xin Mofan Road, Nanjing 210009 (P. R. China).
Email: shaozp@njtech.edu.cn

b. College of Chemical Engineering, Nanjing Tech University, No. 5 Xin Mofan Road, Nanjing 210009 (P. R. China).

c. Center for Innovative Fuel Cell and Battery Technologies, School of Materials Science and Engineering, Georgia Institute of Technology, Atlanta, GA 30332 (USA).
Email: meilin.liu@mse.gatech.edu

d. College of Energy, Nanjing Tech University, No. 5 Xin Mofan Road, Nanjing 210009 (P. R. China).

e. Department of Chemical Engineering, Curtin University, Perth, Western Australia 6845 (Australia).

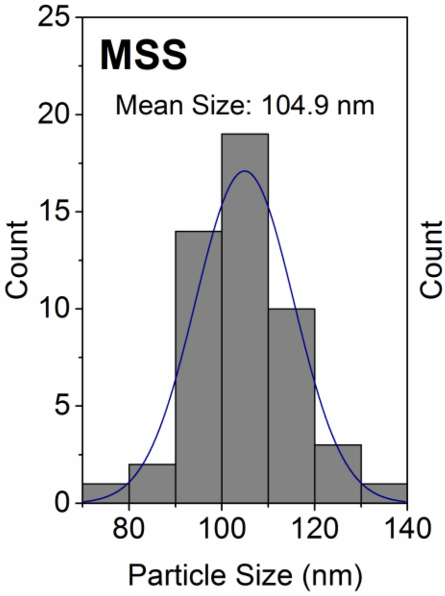

Fig. S1 Particle size distributions of MSS templates and HICSs.

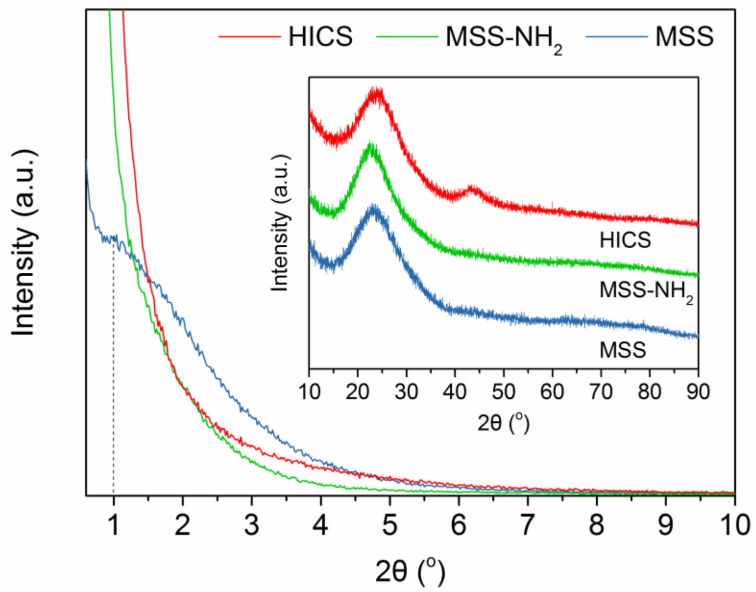

Fig. S2 Low-angle and wide-angle XRD patterns of MSSs, MSSs-NH_2 and HICSs.

The XRD patterns of the HICSs show a broad profile at a 2-theta of approximately 23°, corresponding to the (0 0 2) interlayer reflection, and another peak at a 2-theta of approximately 43°, corresponding to the (1 0 0) in-plane scattering, which indicates a turbostratic type of carbon.[S1-S3]

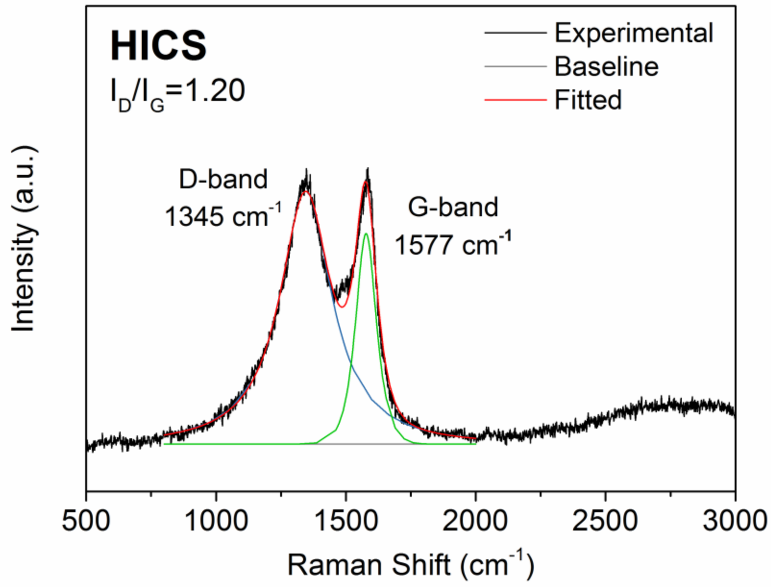

Fig. S3 Raman spectrum of HICSs.

The Raman spectrum of the HISCs shows a D-band at 1345 cm^{-1}, a G-band at 1577 cm^{-1} and a small modulated bump from 2400 to 3000 cm^{-1}. The G-band position, the I_D/I_G value of 1.20 and the absence of well-defined second-order Raman peaks also indicates the turbostratic nature of the HICSs.[S4]

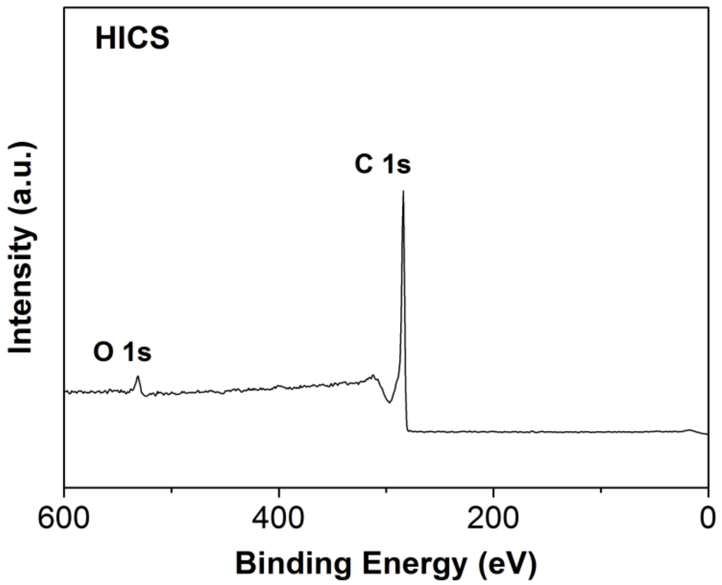

Fig. S4 XPS spectrum of HICS.

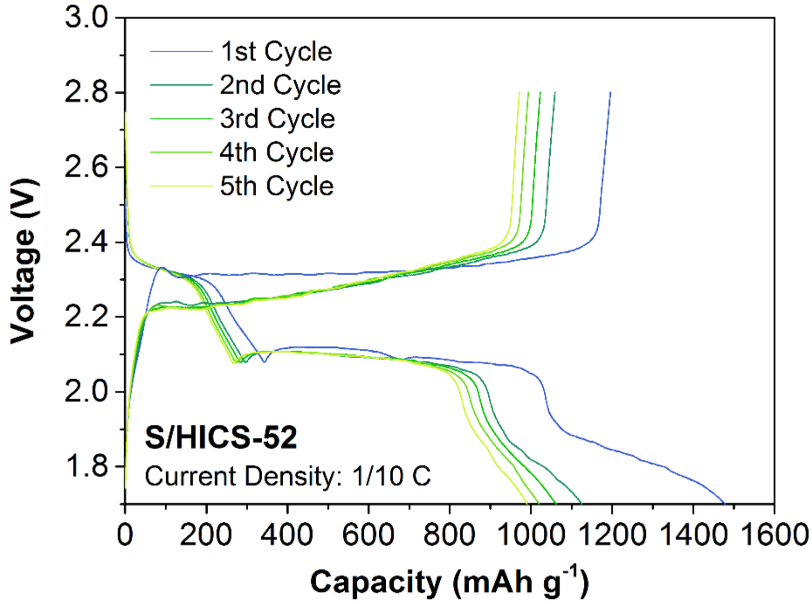

Fig. S5 First five galvanostatic discharge-charge profiles of S/HICS-52 at 1/10 C.

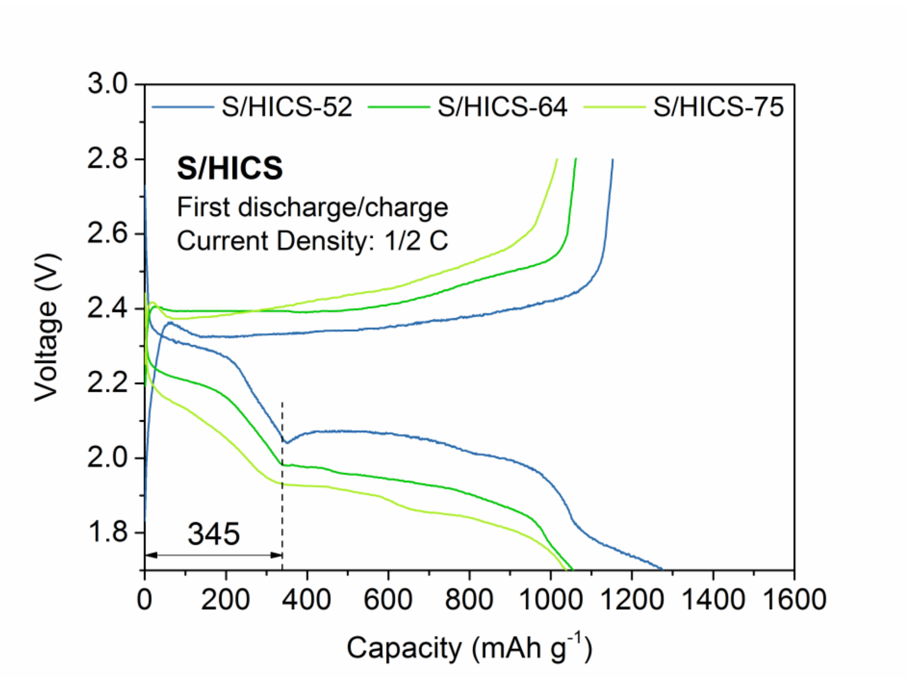

Fig. S6 Initial galvanostatic discharge-charge profile of S/HICS with different sulfur contents at 1/2 C.

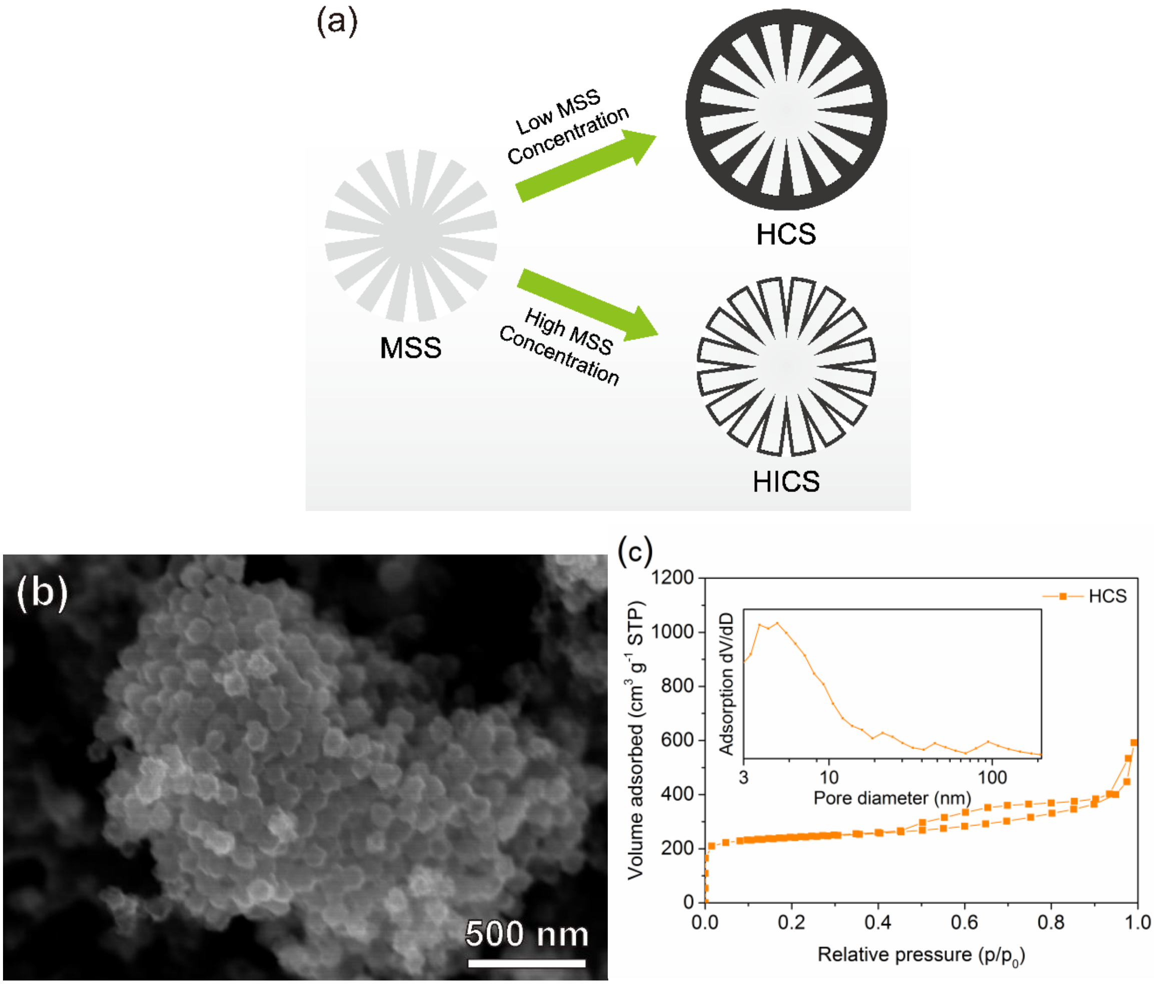

Fig. S7 a) Illustration of comparison for HCS and HICS; b) SEM image of HCS and c) N_2 adsorption-desorption isotherms of HCS (the inset image possesses a PSD from the adsorption branch).

As the concentration of MSS template decreased during the hydrothermal pyrolysis process (other conditions unchanged), the thickness of the carbon shell increased, resulting in the diminishing or vanishing of the external cone-like cavities. The as-prepared HCS had a typical spherical morphological structure, with a diameter and specific surface area similar to that of HICS.

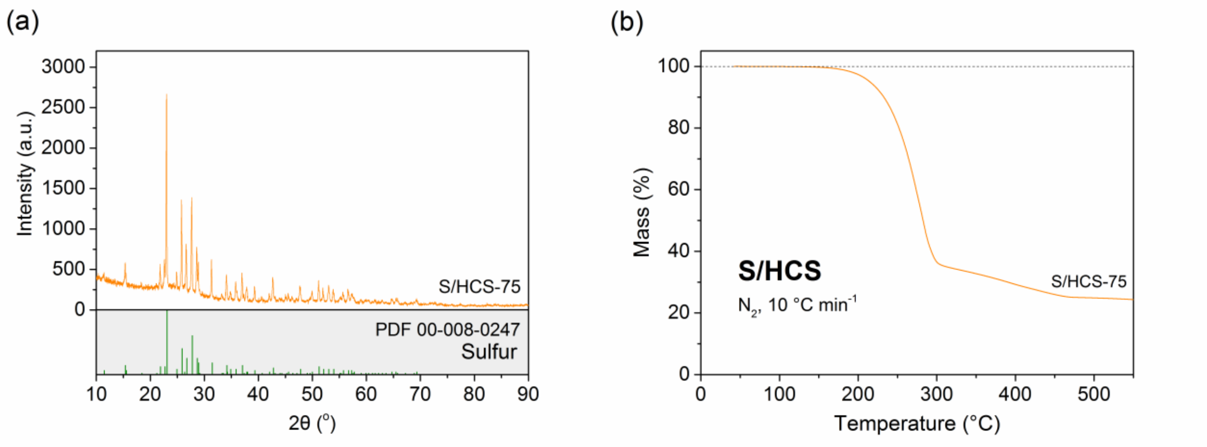

Fig. S8 a) XRD pattern and b) TGA curves of S/HCS-75.

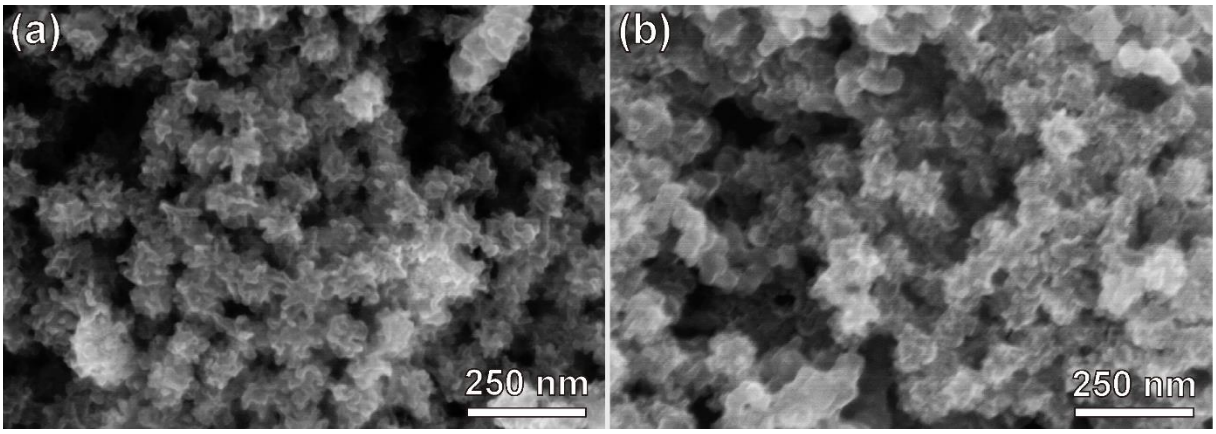

Figure S9 SEM images of a) S/HICS-52 and b) S/HICS-75 cathode after 800 cycles.

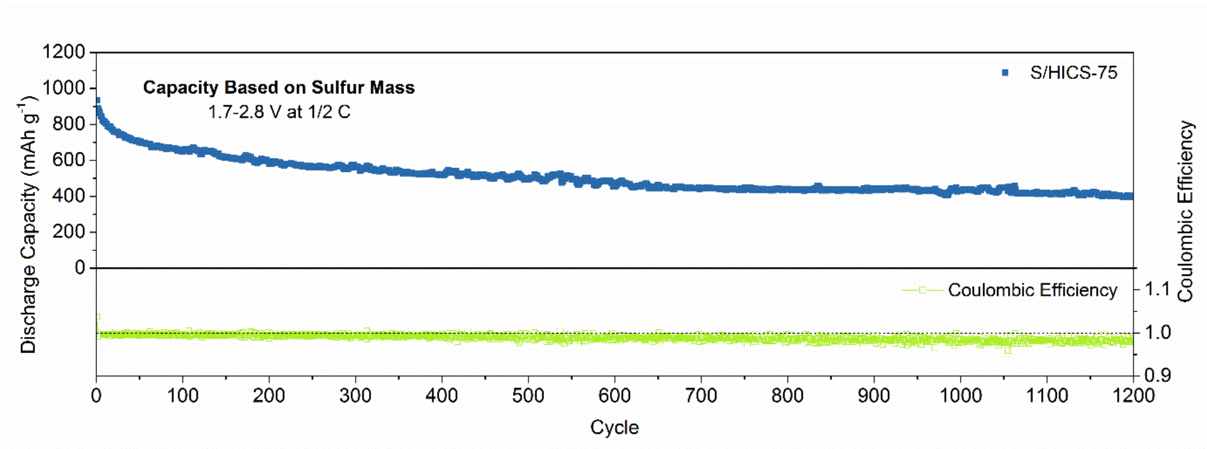

Figure S10 Cycle life and Coulombic efficiency of S/HICS-75 at 1/2 C for 1200 cycles.

Table S1 Physical Properties of MSS and HICS

Sample	$a_{s,BET}$ $m^2\ g^{-1}$	V_{Total}[a] $cm^3\ g^{-1}$	$V_{Meso\text{-}Macro}$[b] $cm^3\ g^{-1}$
HICS	1405	3.72	3.42
MSS	950	2.86	2.78

[a] Gurvich total pore volume (P/P_0 = 0.99); [b] Based on BJH method calculating from p/p_0 between 0.35 and 0.99.

Table S2 Physical Properties of S/HICS Composites

Sample	S Content	S/C	$a_{s,BET}$ $m^2\ g^{-1}$	V_{Total} $cm^3\ g^{-1}$
HICS	0	0	1405	3.72
S/HICS-52	52%	~1:1	147	0.95
S/HICS-64	64%	~2:1	95	0.78
S/HICS-75	75%	~3:1	45	0.38
S/HICS-86	86%	~6:1	16	0.12

NOTE: Owing to the volatility of the sulfur, it was impossible to evacuating the samples at high temperature before the N_2 adsorption-desorption measurements. The pretreatment temperature was reduced to 60 °C for samples with elemental sulfur.

Table S3 Performance comparison of S/HICS with other high-performance cathodes with a porous carbon sphere conductive framework

Conductive Framework	Sulfur Content	1st Discharge Capacity (mAh g^{-1})	Cycling Capacity (mAh g^{-1})	Rate, Voltage Range & Cycles	Ref.
HICS	75%	933	650	0.5 C, at 1.7-2.8 V, 100 cycles	this work
Graphene wrapped nitrogen-doped double-shelled HCS	62%	~800	~620	0.5 C, at 1.5-2.8 V, 100 cycles	S5
Mesoporous CS	80%	1127	569	0.2 C, at 1.5-3.0 V, 100 cycles	S6
Hierarchically porous carbon	66%	1640	440	0.1 A g^{-1}, at 1.0-3.0 V, 100 cycles	S7
Porous CS	72%	1033	~600	0.1 C, at 1.5-2.8 V, 50 cycles	S8
Porous HCS	67%	<1100	N/A	0.05 C, at 1.5-3.0 V, 50 cycles	S9
CNTs	50%	~680	524	1.5 A g^{-1}, at 1.5-2.8 V, 100 cycles	S10
Cross-stacked CNT film	60%	~710	~550	0.5 C, at 1.8-2.6 V, 100 cycles	S11
Graphene foam	70%	~400	~300	3.2 A g^{-1}, at 1.5-3.0 V, 100 cycles	S12
Graphene-wrapped PPy	73%	760	~430	0.2 C, at 1.6-3.0 V, 100 cycles	S13

References

[S1] L. Zhao, N. Baccile, S. Gross, Y. Zhang, W. Wei, Y. Sun, M. Antonietti and M.-M. Titirici, *Carbon*, 2010, **48**, 3778.

[S2] Y. H. Qu, Z. A. Zhang, X. W. Wang, Y. Q. Lai, Y. X. Liu and J. Li, *J. Mater. Chem. A*, 2013, **1**, 14306.

[S3] X. Deng, B. Zhao, L. Zhu and Z. Shao, *Carbon*, 2015, **93**, 48.

[S4] A. C. Ferrari and J. Robertson, *Phys. Rev. B*, 2000, **61**, 14095.

[S5] G. Zhou, Y. Zhao and A. Manthiram, *Adv. Energy Mater.*, 2015, **5**, 1402263.

[S6] D. Wang, A. Fu, H. Li, Y. Wang, P. Guo, J. Liu and X. S. Zhao, *J. Power Sources*, 2015, **285**, 469.

[S7] C. Li and L. Yin, *Part. Part. Syst. Charact.*, 2015, **32**, 756.

[S8] X. Zhao, D.-S. Kim, H.-J. Ahn, K.-W. Kim, K.-K. Cho and J.-H. Ahn, *Mater. Res. Bull.*, 2014, **58**, 204.

[S9] K. Zhang, Q. Zhao, Z. Tao and J. Chen, *Nano Res.*, 2013, **6**, 38.

[S10] G. Zhou, D.-W. Wang, F. Li, P.-X. Hou, L. Yin, C. Liu, G. Q. Lu, I. R. Gentle and H.-M. Cheng, *Energ. Environ. Sci.*, 2012, **5**, 8901.

[S11] L. Sun, W. Kong, M. Li, H. Wu, K. Jiang, Q. Li, Y. Zhang, J. Wang and S. Fan, *Nanotechnology*, 2016, **27**, 075401.

[S12] K. Xi, P. R. Kidambi, R. Chen, C. Gao, X. Peng, C. Ducati, S. Hofmann and R. V. Kumar, *Nanoscale*, 2014, **6**, 5746.

[S13] X. Zhou, F. Chen and J. Yang, *J. Energy Chem.*, 2015, **24**, 448.